# Isoscalar multipole strength in $^{110}$Cd and $^{116}$Cd

Y.-W. Lui, D. H. Youngblood, Y. Tokimoto, H. L. Clark, and B. John*
*Cyclotron Institute, Texas A&M University, College Station, Texas 77843, USA*
(Received 6 October 2003; published 24 March 2004)

The giant resonance region from 10 MeV$<E_x<$55 MeV in $^{110}$Cd and $^{116}$Cd has been studied with inelastic scattering of 240 MeV $\alpha$ particles at small angles including 0°. In $^{110}$Cd($^{116}$Cd), 88+21−13% (104+23 −13%) of the $E0$, 70+23−18% (92±19%) of the $E1$, 89+25−15% (104+21−12%) of the $E2$, and 85+20 −15% (71±17%) of the $E3$ energy-weighted sum rule were identified.

DOI: 10.1103/PhysRevC.69.034611 PACS number(s): 25.55.Ci, 24.30.Cz, 27.60.+j

## I. INTRODUCTION

The locations of the isoscalar giant monopole resonance (GMR) and giant dipole resonances (ISGDR) are important because their energies can be directly related to the nuclear compressibility and from this the compressibility of nuclear matter ($K_{NM}$) can be obtained [1,2]. Of particular interest is the variation of compressibility with neutron number. Studies of the GMR in the Sn isotopes were carried out a number of years ago [3] to determine the isotopic behavior of the GMR with an emphasis on determining the coefficient of the $(N-Z)/A$ term in the leptodermous expansion. Since that time there are newer calculations with different interactions which should be tested, but these early data have relatively large errors compared to what is possible now. Furthermore, because of the much improved peak to continuum ratio [4] we can now look at the actual distribution of strength as well as the behavior of the ISGDR, which was not possible then. With this in mind, we have studied $^{110}$Cd and $^{116}$Cd with small angle inelastic $\alpha$ scattering at 240 MeV, which has been very useful in obtaining strength distributions of isoscalar electric multipoles in several nuclei [4].

## II. EXPERIMENTAL TECHNIQUE AND DATA ANALYSIS

The experimental technique has been described thoroughly in Ref. [4] and is summarized briefly below. Beams of 240 MeV $\alpha$ particles from the Texas A&M K500 superconducting cyclotron bombarded self-supporting Cd foils 3.9 mg/cm$^2$($^{110}$Cd) and 4.1 mg/cm$^2$($^{116}$Cd) thick, enriched to more than 96% in the desired isotope, located in the target chamber of the multipole-dipole-multipole spectrometer. The horizontal acceptance of the spectrometer was 4° and ray tracing was used to reconstruct the scattering angle. The vertical acceptance was set at ±2°. The focal plane detector measured position and angle in the scattering plane and covered from 47 to 55 MeV of excitation, depending on scattering angle. The out-of-plane scattering angle was not measured. Position resolution of approximately 0.9 mm and scattering angle resolution of about 0.09° were obtained. Cross sections were obtained from the charge collected, target thickness, dead time, and known solid angle. The target thicknesses were measured by weighing and checked by measuring the energy loss of the 240 MeV $\alpha$ beam in each target. The cumulative uncertainties in target thickness, solid angle, etc., result in about a ±10% uncertainty in absolute cross sections. $^{24}$Mg spectra were taken before and after each run with each target and the 13.85±.02 MeV L=0 state [5] was used as a check on the calibration in the giant resonance region.

Sample spectra obtained for $^{110}$Cd are shown in Fig. 1. Those obtained for $^{116}$Cd are similar. The giant resonance peak can be seen extending up past $E_x$=30 MeV. The spectrum was divided into a peak and a continuum, where the

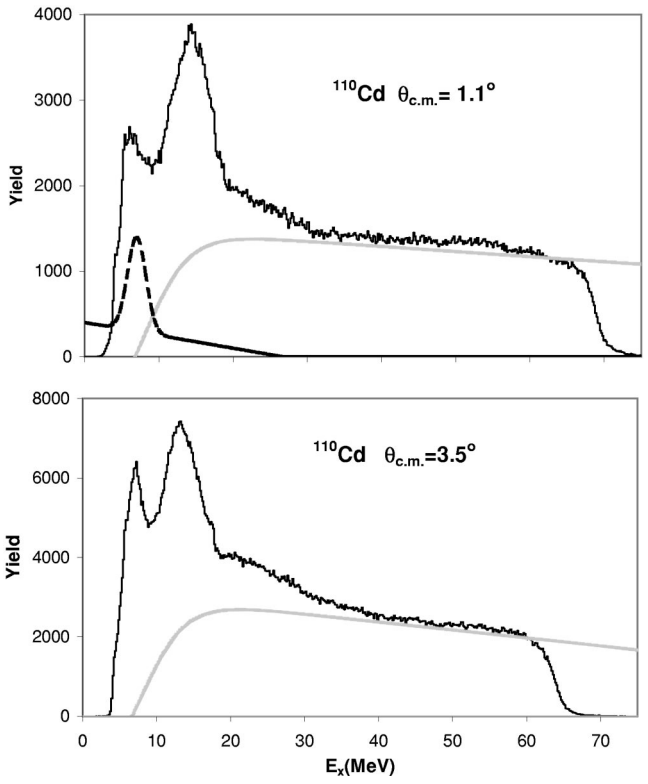


FIG. 1. Inelastic $\alpha$ spectra obtained at two angles for $^{110}$Cd. The thick gray lines show the continuum chosen for the analysis. The dashed line below 10 MeV represents a contaminent peak present at some angles in the spectra taken with the spectrometer at 0°. This was subtracted before the multipole analysis was done.

*Present address: Nuclear Physics Division, Bhabha Atomic Research Center, Mumbai-400085, India.

 

continuum was assumed to have the shape of a straight line at high excitation joining onto a Fermi shape at low excitation to model particle threshold effects [4]. Samples of the continua used are shown in Fig. 1.

### III. MULTIPOLE ANALYSIS

The multipole components of the giant resonance peak were obtained [4] by dividing the peak into multiple regions (bins) by excitation energy and then comparing the angular distributions obtained for each of these bins to distorted wave Born approximation (DWBA) calculations. The uncertainty from the multipole fits was determined for each multipole by incrementing (or decrementing) that strength, then adjusting the strengths of the other multipoles to minimize total $\chi^2$. This continued until the new $\chi^2$ was one unit larger than the total $\chi^2$ obtained for the best fit.

Elastic scattering data were not available for $^{110}$Cd or $^{116}$Cd, so optical model parameters obtained for $^{116}$Sn [6] were used. Single folding density dependent DWBA calculations (as described in Refs. [4,7]) were carried out with Fermi mass distributions for $^{110}$Cd and $^{116}$Cd using $c = 5.3435$ and 5.4164 fm, respectively [8] and $a = 0.523$ fm for both nuclei. The transition densities, sum rules, and DWBA calculations were discussed thoroughly in Ref. [4] and, except for the isoscalar dipole, the same expressions and techniques were used in this work. The transition density for inelastic $\alpha$ particle excitation of the ISGDR given by Harakeh and Dieperink [9] (and described in Ref. [4]) is for only one magnetic substate, so that the transition density given in Ref. [9] must be multiplied by the square root of 3 in the DWBA calculation.

A sample of the angular distributions obtained for the giant resonance (GR) peak and the continuum are shown for $^{110}$Cd in Fig. 2. Fits to the angular distributions were carried out with a sum of isoscalar $0^+, 1^-, 2^+, 3^-$, and $4^+$ strengths. The isovector giant dipole resonance contributions were calculated from the known distribution [10] for natural Cd and held fixed in the fits. Sample fits obtained, along with the individual components of the fits, are shown superimposed on the data in Fig. 2. The continuum distributions are similar over the entire energy range, whereas the angular distributions of the cross sections for the peak change as the contributions of different multipoles dominate in different energy regions.

Several analyses were carried out to assess the effects of different choices of the continuum on the resulting multipole distributions. Analyses were made using continua chosen with several different criteria [e.g., (a) using a slope for the linear part which did not quite match the data at high excitation, (b) lowering the continuum so that it was always below the data, (c) changing the low energy cutoff and slope of the continuum, and (d) deliberately altering the continuum slope and/or amplitude at only selected angles]. The strength distributions obtained from these analyses were then averaged, and errors calculated by adding the errors obtained from the multipole fits in quadrature to the standard deviations between the different fits. The (isoscalar) $E0$, $E1$, $E2$ and $E3$ multipole distributions obtained are shown in Figs. 3

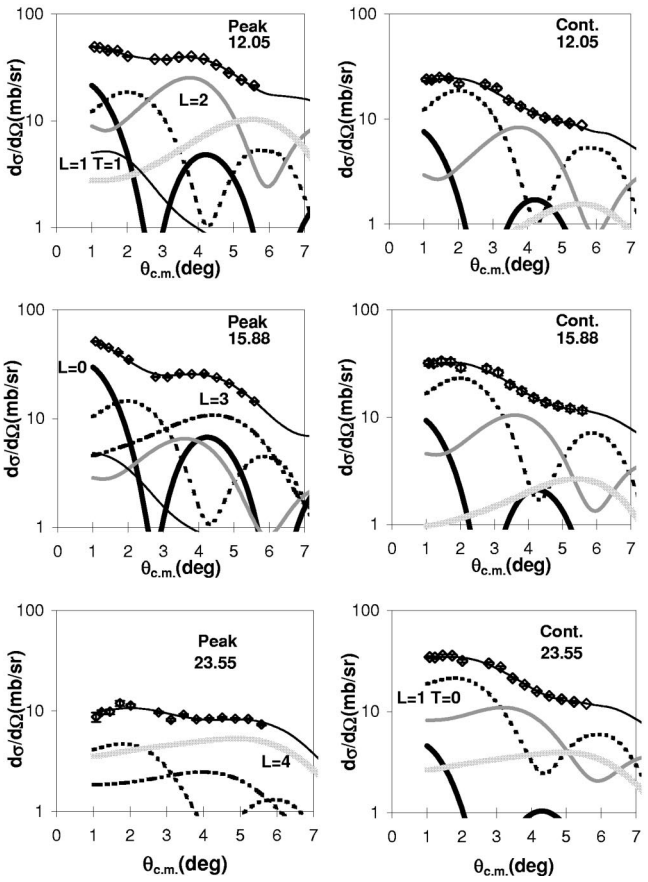


FIG. 2. The angular distributions of the $^{110}$Cd cross sections for a 960 keV wide bin centered at the excitation energy indicated in the figure (in MeV) for inelastic $\alpha$ scattering for three excitation ranges of the GR peak and the continuum. The lines through the data points indicate the multipole fits. Contributions of each multipole are shown. The statistical errors are smaller than the data points.

and 4 and the energy moments and sum rule strengths obtained are summarized in Tables I and II. Due to the limited angular range of the data, $E4$ strength could not be distinguished from higher multipoles and those results are not included. Single Gaussians were also fit to the $E0$, $E2$, and $E3$ distributions and two Gaussians were fit to the $E1$ distribution. These are shown in Figs. 3 and 4 and the parameters obtained are listed in Tables I and II.

### IV. DISCUSSION

In both nuclei, strength consistent with 100% of the energy-weighted sum rule (EWSR) was located for both $E0$ and $E2$ transitions, concentrated in an almost Guassian peak but with some tailing at low excitation. The uncertainties in the region around $E_x = 10$ MeV are larger than at higher excitation due to a rapidly varying solid angle near the low energy cutoff in the detector and the uncertainty caused by the presence of some real background in this region (seen as a dashed peak in Fig. 1). The only previous measurements of $E0$ and $E2$ GR strength in the Cd isotopes was by Buenerd [11], who used inelastic $^3$He scattering at small angles and fit

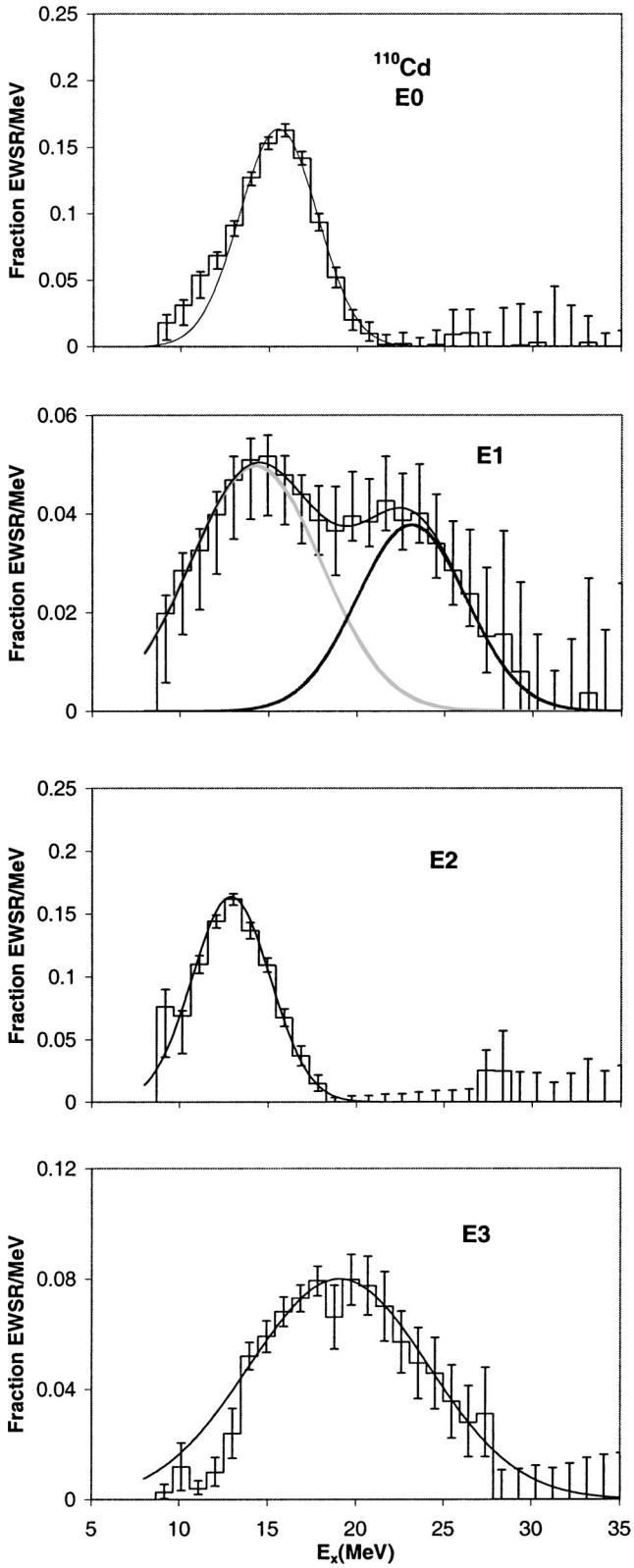


FIG. 3. Strength distributions obtained for $^{110}$Cd are shown by the histograms. Error bars represent the uncertainty due to the fitting of the angular distributions and different choices of the continuum as described in the text. The smooth lines show Gaussian fits.

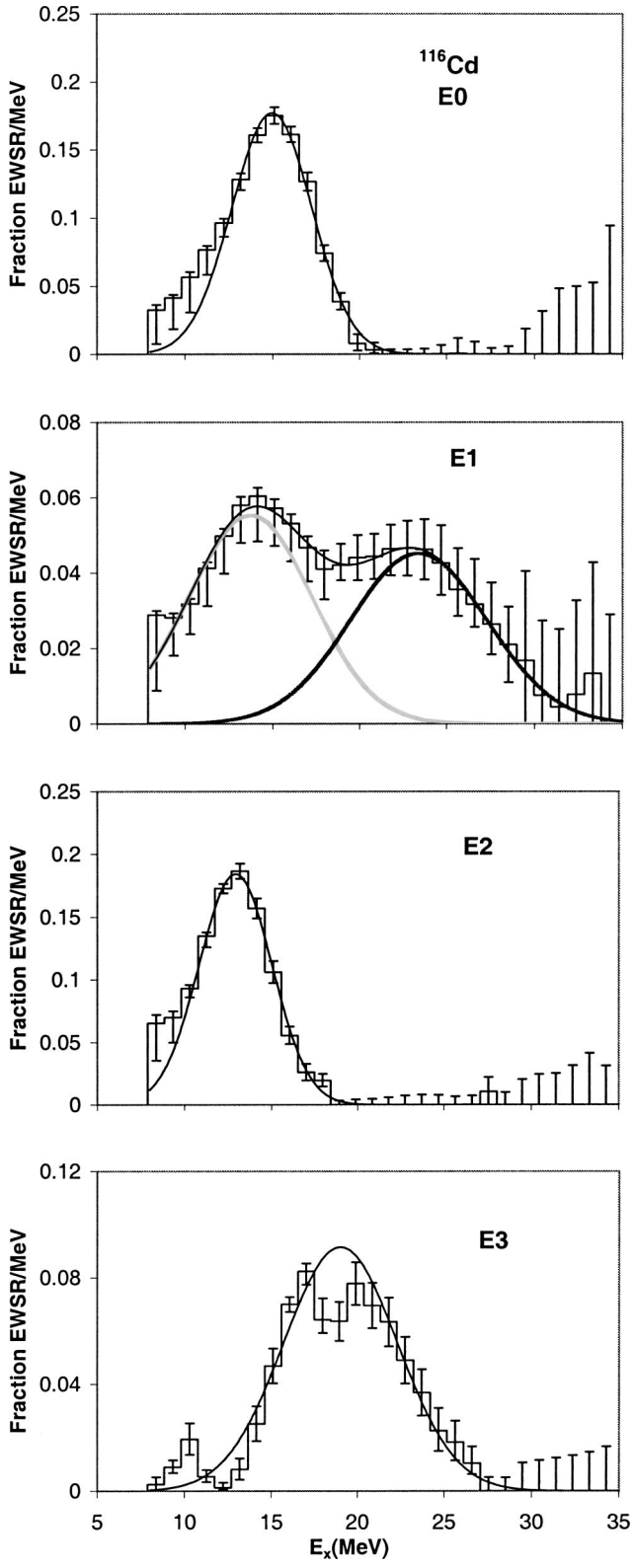


FIG. 4. Strength distributions obtained for $^{116}$Cd are shown by the histograms. Error bars represent the uncertainty due to the fitting of the angular distributions and different choices of the continuum as described in the text. The smooth lines show Gaussian fits.

TABLE I. Paramameters obtained for isoscalar multipoles in $^{110}$Cd.

| | | | | | | | | | | | | |
|---|---|---|---|---|---|---|---|---|---|---|---|---|
| Moments | | | | | | | | | | | | |
| | $E0$ | −Error | +Error | $E1$ | −Error | +Error | $E2$ | −Error | +Error | $E3$ | −Error | +Error |
| $m_1$ (Frac EWSR) | 0.88 | 0.13 | 0.21 | 0.70 | 0.18 | 0.23 | 0.89 | 0.15 | 0.25 | 0.85 | 0.15 | 0.20 |
| $m_1/m_0$ (MeV) | 15.12 | 0.11 | 0.30 | 16.90 | 0.21 | 0.67 | 13.11 | 0.14 | 0.66 | 18.73 | 0.10 | 0.28 |
| rms width (MeV) | 2.16 | 0.08 | 0.12 | 5.54 | 0.27 | 1.72 | 1.73 | 0.10 | 0.45 | 4.15 | 0.21 | 1.16 |
| $(m_3/m_1)^{1/2}$ (MeV) | 15.58 | 0.09 | 0.40 | | | | | | | | | |
| $(m_1/m_{-1})^{1/2}$ (MeV) | 14.96 | 0.12 | 0.13 | | | | | | | | | |
| Gaussian fits | | | | | | | | | | | | |
| | $E0$ | −Error | +Error | $E1$ $Pk1$ | −Error | +Error | $E1$ $Pk2$ | −Error | +Error | $E2$ | −Error | +Error | $E3$ | −Error | +Error |
| Centroid (MeV) | 15.71 | 0.11 | 0.11 | 14.47 | 0.47 | 0.44 | 23.30 | 0.48 | 0.55 | 13.09 | 0.13 | 0.14 | 19.26 | 0.29 | 0.31 |
| FWHM (MeV) | 5.18 | 0.17 | 0.16 | 8.70 | 0.87 | 0.87 | 7.32 | 0.78 | 1.09 | 5.18 | 0.41 | 0.09 | 12.00 | 2.96 | 0.09 |
| Fraction EWSR | 0.86 | 0.10 | 0.10 | 0.42 | 0.11 | 0.11 | 0.28 | 0.11 | 0.11 | 0.85 | 0.13 | 0.10 | 0.96 | 0.22 | 0.10 |

| Buenerd (Ref. [11]) | $E0$ | −Error | +Error | $E2$ | −Error | +Error |
|---|---|---|---|---|---|---|
| Centroid (MeV) | 15.95 | 0.25 | 0.25 | 13.3 | 0.25 | 0.25 |
| FWHM (MeV) | 4.15 | 0.25 | 0.25 | 4 | 0.25 | 0.25 |
| Fraction EWSR | 0.36 | | | 0.6 | | |

TABLE II. Paramameters obtained for isoscalar multipoles in $^{116}$Cd.

| | | | | | | | | | | | | |
|---|---|---|---|---|---|---|---|---|---|---|---|---|
| | | | | Moments | | | | | | | | |
| | $E0$ | −Error | +Error | $E1$ | −Error | +Error | $E2$ | −Error | +Error | $E3$ | −Error | +Error |
| $m_1$ (Frac EWSR) | 1.04 | 0.13 | 0.23 | 0.92 | 0.19 | 0.19 | 1.04 | 0.12 | 0.21 | 0.71 | 0.17 | 0.17 |
| $m_1/m_0$ (MeV) | 14.50 | 0.16 | 0.32 | 16.87 | 0.20 | 0.51 | 12.50 | 0.16 | 0.50 | 18.28 | 0.09 | 0.25 |
| rms width (MeV) | 2.26 | 0.10 | 0.12 | 6.46 | 0.43 | 1.15 | 2.30 | 0.30 | 0.30 | 3.76 | 0.11 | 0.90 |
| $(m_3/m_1)^{1/2}$ (MeV) | 15.02 | 0.12 | 0.37 | | | | | | | | | |
| $(m_1/m_{-1})^{1/2}$ (MeV) | 14.31 | 0.17 | 0.20 | | | | | | | | | |

| | | | | | | | | | | | | | | | |
|---|---|---|---|---|---|---|---|---|---|---|---|---|---|---|---|
| | | | | | Gaussian fits | | | | | | | | | | |
| | $E0$ | −Error | +Error | $E1$ $Pk1$ | −Error | +Error | $E1$ $Pk2$ | −Error | +Error | $E2$ | −Error | +Error | $E3$ | −Error | +Error |
| Centroid (MeV) | 15.17 | 0.11 | 0.12 | 13.94 | 0.30 | 0.26 | 23.58 | 0.42 | 0.42 | 13.13 | 0.12 | 0.12 | 19.21 | 0.61 | 0.81 |
| FWHM (MeV) | 5.40 | 0.14 | 0.16 | 8.31 | 0.46 | 0.59 | 9.22 | 0.72 | 0.92 | 4.94 | 0.16 | 0.18 | 7.80 | 1.00 | 0.60 |
| Fraction EWSR | 1.00 | 0.11 | 0.11 | 0.46 | 0.11 | 0.11 | 0.44 | 0.11 | 0.11 | 0.95 | 0.11 | 0.11 | 0.75 | 0.23 | 0.22 |

| Buenerd (Ref. [11]) | $E0$ | −Error | +Error | $E2$ | −Error | +Error |
|---|---|---|---|---|---|---|
| Centroid (MeV) | 15.75 | 0.25 | 0.25 | 12.95 | 0.25 | 0.25 |
| FWHM (MeV) | 3.4 | 0.3 | 0.3 | 4 | 0.3 | 0.3 |
| Fraction EWSR | 0.53 | | | 0.88 | | |

the data with two Gaussians, one for $E0$ and one for $E2$. However, after a later $\alpha$ scattering study on Ni, Mo, and Sn where they found substantially more $E0$ strength and larger experimental widths than in their $^3$He scattering [12], they concluded that their analysis of $^3$He scattering did not identify all the $E0$ strength. They identified only 36% and 53% of the $E0$ EWSR in $^{110}$Cd and $^{116}$Cd, respectively, so that a direct comparison of their energies to our results would not be meaningful. They did locate 60% and 88% of the $E2$ strength in $^{110}$Cd and $^{116}$Cd, respectively, and their energies agree within errors with those obtained from our Gaussian fits. We obtain somewhat larger widths and strengths than they report.

There have been no previous reports of isoscalar dipole or $3\hbar\omega$ $E3$ strength in the Cd isotopes. The isoscalar dipole resonance is known to consist of two components [6,13,14] and this is seen clearly in Figs. 3 and 4. In $^{110}$Cd, $70+23-18\%$ of the $E1$ sum rule was identified and in $^{116}$Cd $92\pm19\%$ was identified. The lower components have similar widths and strengths in both nuclei, but the higher component is substantially weaker and narrower in $^{110}$Cd. This may be an artifact of the experiment as we find that the multipole analysis has large errors above $E_x=30$ MeV. The (apparent) lower strength could be because we are missing strength lying at higher excitation in $^{110}$Cd. $E3$ strength in nuclei is split into $1\hbar\omega$ and $3\hbar\omega$ components [15] and some portion of the $1\hbar\omega$ strength is apparent in both nuclei around 10 MeV. Around 75% of the $E3$ strength should be in the $3\hbar\omega$ component, and this is consistent with the $E3$ strength observed in both nuclei.

There are no specific calculations for $E0$ strength in the Cd isotopes, however, Nayak *et al.* [16] have carried out Hartree-Fock random phase approximation calculations with several Skyrme or Skyrme-like interactions and parametrized the results in terms of the Leptodermous expansion. Farine, Pearson, and Tondeur [17] carried out a study using modified Skyrme interactions (parametrized with the leptodermous expansion) designed to explore how the effective $K_{\rm NM}$ for an interaction might be changed while still providing breathing mode energies consistent with experimental results. Chossy and Stocker [18] have carried out a similar parametrization for several relativistic parameter sets. $E0$ energies calculated with relativistic and nonrelativistic interactions are compared to the experimental energies for the Cd isotopes in the top panel of Fig. 5. The experimental energies are slightly below energies obtained with calculations for interactions for which $K_{\rm NM}\sim211-216$ MeV. This is somewhat lower than $K_{\rm NM}\sim231$ MeV suggested by energies for a number of other nuclei [19] including $^{116}$Sn. The (Gaussian centroid) energy of the GMR in $^{116}$Sn [19] is $830\pm160$ keV higher than in $^{116}$Cd, whereas the parametrizations in Refs. [16–18] lead to predictions of differences from 100–300 keV, much less than the experimental value. These results suggest that the GMR energies in the Cd isotopes are abnormally low compared to the closed shell nuclei of similar mass.

The energy difference between the two Cd isotopes is much better determined than the actual energy, as systematic errors (such as strength errors at around 10 MeV due to background, detector threshold effects, continuum choices) should be similar for both nuclei. This difference might be expected to depend mostly on the symmetry term [dependent on $(N-Z)/A$] in the leptodermous expansion, and that is the largest contribution. The lower panel compares calculations for the Cd energy difference using the parametrizations of Nayak *et al.*, Chossy and Stocker, and Farine, Pearson, and Tondeur with the experimental difference. Except for the S3 interaction ($K_{\rm NM}=333$ MeV), each of the nonrelativistic interactions used by Nayak *et al.* results in an energy difference much lower than the experimental results, while the energy differences calculated with the relativisitc interactions fall in or very near the experimental range. The results from the modified Skyrme interactions with $200\leqslant K_{\rm NM}\leqslant240$ MeV are consistent with the data, while that for SkK180 is too low.

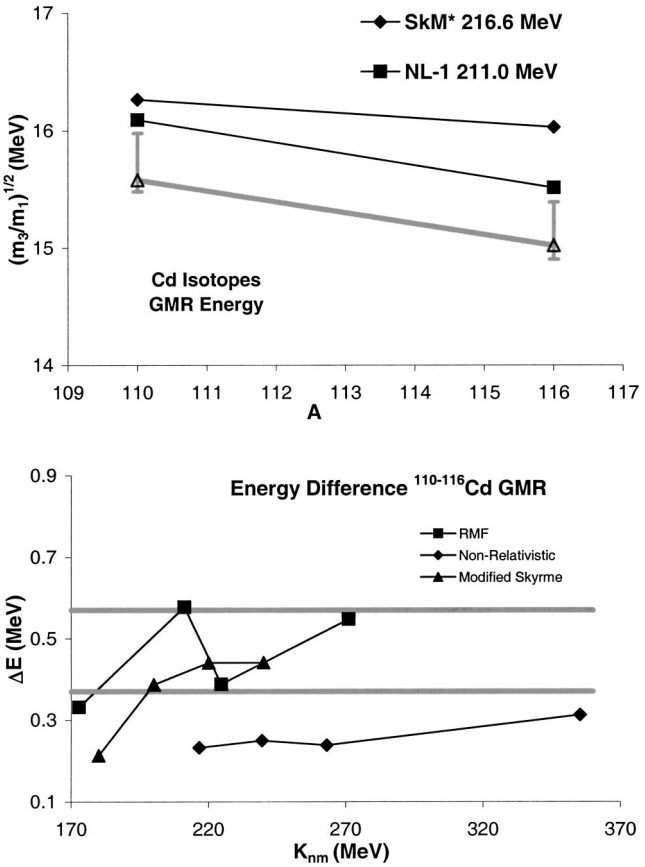


FIG. 5. (Top) GMR energies calculated with the relativistic mean field parametrization [18] and nonrelativistic parametrizations [16] are compared to the experimental energies shown in gray. The error bars include systematic errors. (Bottom) The difference in GMR energies between $^{110}$Cd and $^{116}$Cd calculated with the relativistic mean field parametrization [18] and nonrelativistic parametrizations [16] included the modified Skyrme [17] are compared to the experimental difference whose limits are indicated by the horizontal gray lines. The experimental range shown is an average of the values obtained from the Gaussian fits and the energy moments, and includes statistical errors, but not systematic errors.

## V. CONCLUSIONS

Most of the expected isoscalar $E0-E3$ strength in $^{110}$Cd and $^{116}$Cd has been identified. Some of the $E1$ strength in

$^{110}$Cd was not located, and may be located above $E_x = 30$ MeV where the errors of the analysis are larger. Predictions using relativistic and nonrelativistic (Skyrme or Skyrme-like) interactions with $K_{NM} \sim 211-216$ MeV result in energies slightly above the experimental energies. The energy difference between the $E0$ positions in $^{110}$Cd and $^{116}$Cd is consistent with the relativistic calculations and with calculations using modified Skyrme interactions differing from Skyrme ones primarily in the behavior of the density dependence to provide a more reliable extrapolation to neutron rich systems.

## ACKNOWLEDGMENTS

This work was supported in part by the U.S. Department of Energy under Grant No. DE-FG03-93ER40773 and by The Robert A. Welch Foundation.

[1] J. P. Blaizot, Phys. Rep. **64**, 171 (1980).
[2] S. Stringari, Phys. Lett. **108B**, 232 (1982).
[3] S. Shlomo and D. H. Youngblood, Phys. Rev. C **47**, 529 (1993), and references therein.
[4] D. H. Youngblood, Y.-W. Lui, and H. L. Clark, Phys. Rev. C **65**, 034302 (2002); **63**, 067301 (2001); **60**, 014304 (1999).
[5] K. van der Borg, M. N. Harakeh, and A. van der Woude, Nucl. Phys. **A365**, 243 (1981).
[6] H. L. Clark, Y.-W. Lui, and D. H. Youngblood, Phys. Rev. C **57**, 2887 (1998).
[7] G. R. Satchler and Dao T. Khoa, Phys. Rev. C **55**, 285 (1997).
[8] G. Fricke, C. Bernhardt, K. Heilig, L. A. Schaller, L. Schellenberg, E. B. Shera, and C. W. DeJager, At. Data Nucl. Data Tables **60**, 177 (1995).
[9] M. N. Harakeh and A. E. L. Dieperink, Phys. Rev. C **23**, 2329 (1981).
[10] S. S. Dietrich and B. L. Berman, At. Data Nucl. Data Tables **38**, 199 (1988).
[11] M. Buenerd, in *Proceedings of International Symposium on Highly Excited States and Nuclear Structure, Orsay, France*, edited by N. Marty and N. van Giai [J. Phys. (Paris), Colloq. **45**, C4-115 (1984)].
[12] G. Duhamel, M. Buenerd, P. de Saintingnon, J. Chauvin, D. Lebrun, Ph. Martin, and G. Perrin, Phys. Rev. C **38**, 2509 (1988).
[13] G. Colo, N. Van Giai, P. F. Bortignon, and M. R. Quaglia, Phys. Lett. B **485**, 362 (2000).
[14] D. Vretenar, A. Wandelt, and P. Ring, Phys. Lett. B **487**, 334 (2000).
[15] J. M. Moss, D. H. Youngblood, C. M. Rozsa, D. R. Brown, and J. D. Bronson, Phys. Rev. Lett. **37**, 816 (1976).
[16] R. C. Nayak, J. M. Pearson, M. Farine, P. Gleissl, and M. Brack, Nucl. Phys. **A516**, 62 (1990).
[17] M. Farine, J. M. Pearson, and F. Tondeur, Nucl. Phys. **A615**, 137 (1997).
[18] T. V. Chossy and W. Stocker, Phys. Rev. C **56**, 2518 (1997).
[19] D. H. Youngblood, H. L. Clark, and Y.-W. Lui, Phys. Rev. Lett. **82**, 691 (1999).